REGULAR PAPER

J. Physiol. Sci. Vol. 58, No. 5; Oct. 2008; pp. 349–355
Online Oct. 7, 2008; **doi:10.2170/physiolsci.RP004908**

Histological Skeletal Muscle Damage and Surface EMG Relationships Following Eccentric Contractions

Yutaka KANO[1], Kazumi MASUDA[2], Hirotaka FURUKAWA[1], Mizuki SUDO[1], Kazuyuki MITO[3], and Kazuyoshi SAKAMOTO[3]

[1]Department of Applied Physics and Chemistry, University of Electro-Communications, Chofugaoka, Chofu, Tokyo, 182-8585 Japan;
[2]Department of Health Education, Faculty of Education, Kanazawa University, Kakuma, Kanazawa, Ishikawa, 920-1192 Japan; and
[3]Department of Systems Engineering, University of Electro-Communications, Chofugaoka, Chofu, Tokyo, 182-8585 Japan

Abstract: This study examined the effects of a different number of eccentric contractions (ECs) on histological characteristics, surface electromyogram (EMG) parameters (integral EMG, iEMG; muscle fiber conduction velocity, MFCV; and action potential waveform), and isometric peak torque using the rat EC model. Male Wistar rats (n = 40) were anesthetized, and ECs were initiated in the tibialis anterior muscle via electrical stimulation while the muscle was being stretched by electromotor. The rats were grouped according to the number of ECs (EC1, EC5, EC10, EC20, EC30, EC40, and EC100). Three days after the ECs, surface EMG signals and isometric peak torque were measured during evoked twitch contractions via electrical stimulation of the peroneal nerve. The muscle damage was evaluated from hematoxylin-eosin (HE) stained cross sections as a relative number of damaged fibers to intact fibers. Intense histological muscle damage (approximately 50% to 70% of the fiber), loss of isometric peak torque, disturbance of action potential waveform, and depression of iEMG (approximately –60% to –70%) were observed at EC20, EC30, EC40, and EC100. On the other hand, the MFCV did not change in any EC group. Although muscle damage and pathological surface EMG signals were not found at EC10, isometric peak torque was reduced significantly. In conclusion, the extent of histological muscle damage is not proportionally related to the number of ECs. Muscle damage was reflected by iEMG and action potential waveforms, but not by MFCV, which remained unaffected even though approximately 50% to 70% of the fiber demonstrated injury.

Key words: electromyography, muscle fiber conduction velocity, integrated EMG, histology, electrical stimulation.

Eccentric muscle contractions (ECs) are characterized by higher muscle forces and greater mechanical efficiency compared with isometric and concentric muscle contractions [1]. Also, ECs lead to muscle damage, such as Z-band streaming, A-band disorganization, swelling, and hypercontraction [2, 3]. Quantification of muscle damage by histological observation in human skeletal muscle is problematic. Specifically, muscle biopsies require surgical intervention, and the small tissue specimens obtained are not very likely to be representative of the whole muscle. In contrast, analysis by surface electromyography is noninvasive, and its signals have been used to evaluate, for example, muscle fatigue [4–7] and neuromuscular diseases [8, 9]. Human studies have found that the characteristics of surface EMG signals are modified by EC [10–15]. Berry *et al.* [15] and Kroon and Naeije [13] observed that an increase in EMG activity is needed to produce the same level external force after ECs. On the other hand, Day *et al.* [11] reported that no changes in EMG activity were recorded following ECs. Also, significant decreases in the mean frequency of the EMG were observed after a few days of EC [10–15].

Since the surface EMG represents the sum of a large number of motor unit action potentials [5], it is assumed that EMG alterations are a reflection of the extent of structural muscle damage. However, there is no research that elucidates the relationship between EMG alterations and quantitative analysis of muscle damage. The aim of the present investigation was to examine the effects of different numbers of ECs on histological characteristics, surface EMG parameters (integral EMG, iEMG; muscle fiber conduction velocity, MFCV; and action potential waveform), and isometric peak torque. We hypothesized that the amount of muscle damage increases progressively with the number of ECs, and the extent of muscle fiber damage is reflected by EMG parameters and muscle force.

MATERIALS AND METHODS

Experimental animals. Forty male Wistar rats were used in the present study (Japan SLC, Inc., Shizuoka Lab. Ani-

Received on Apr 1, 2008; accepted on Sep 1, 2008; released online on Oct 7, 2008; doi:10.2170/physiolsci.RP004908
Correspondence should be addressed to: Yutaka Kano, Departments of Applied Physics and Chemistry, University of Electro-Communications, Chofu, Tokyo, 182-8585 Japan. E-mail: kano@pc.uec.ac.jp

mal Center, body weight = 284.7 ± 16.9 g, 13 weeks old). All rats were housed in a temperature-controlled room at 22 ± 2°C with a light-dark cycle of 12 h and maintained on rat chow and water ad libitum. All procedures performed in this study conformed to the Guiding Principles for the Care and Use of Animals in the Field of Physiological Sciences (published by the Physiological Society of Japan). All procedures for surgery, muscle stimulation, and muscle dissections were performed under pentobarbital anesthesia (70 mg kg^{-1} body mass).

Eccentric contraction (EC) protocol. The rats were divided into 7 groups (each group, n = 4 to 7) according to the number of ECs: EC1 (n = 6), EC5 (n = 6), EC10 (n = 7), EC20 (n = 7), EC30 (n = 4), EC40 (n = 4), and EC100 (n = 6). The ECs were evoked according to previously described methods [16]. The right tibialis anterior muscles (TA) were stimulated electrically via a surface electrode (10 V stimulation, 100 Hz frequency, and 700 ms stimulation period, i.e., 70 pulses). The surface electrodes (A-20, Nihon Kohden, Japan) were positioned in a distal and proximal part of the TA. In preliminary experiments and our previous study [16], we confirmed that maximum muscle tension was achieved by electrical stimulation of a surface electrode (100 Hz, <10 V). In the resting condition before EC, the right foot was attached to the clamp unit, and the plate was connected to the electromotor system (Model RU-72, NEC Medical Systems, Japan). The right ankle joint was maintained at 50 degrees as the initial angle. During electrostimulation of the TA, the electromotor was rotated at an angular velocity of 260 degrees s^{-1} by which the dorsiflexor muscle group was lengthened to 180 degrees of the ankle joint. The generated muscle EC tension was monitored using a strain gauge that was incorporated into the plate fixing the foot. The strain gauge was calibrated using precision calibration weights that spanned the expected strains expected during the experiments. The TA of the left leg was not stimulated at all, but served as a contralateral control. EC1, EC5, EC10, EC20, EC30, EC40, and EC100 denote the number of contractions performed by the stimulated TA muscles. Because the EC may induce muscle soreness, the animals are monitored once per day after EC to check activity level and feed intake. Neither abnormal ambulatory activity nor pathological sequelae were observed following EC.

Analysis of EMG signal and peak twitch force. Three days after EC, all rats were subjected to 20 electrically evoked twitch contractions via peroneal nerve stimulation (supramaximal voltage: 1–2 V) with a single 200 μs square wave (between contractions interval = 30 s). During contraction, isometric peak tension and surface myoelectric signals were recorded in the control-TA (left leg) and EC-TA (right leg). Before stimulation, the ankle and knee joint angles were clamped at 90 degrees on the exercise apparatus (Model RU-72, NEC Medical Systems, Tokyo, Japan) (Fig. 1). An array-type surface electrode was placed on the TA parallel to the direction of the muscle fibers. The surface electrode for recording action potentials was composed of seven Ag/AgCl wires each 4.0 mm long and 1.0 mm wide (TN-200-214, Unique Medical, Tokyo, Japan) (Fig. 1). The array was mounted on a rubber plate with an interelectrode distance of 2.0 mm. The myoelectric signals were transferred to a microcomputer using data acquisition software (Chart Ver. 3.6.3) at a sampling frequency of 10 kHz. The muscle fiber conduction velocity (MFCV) was calculated from the time difference of the action potentials between neighboring channels [17]. When the action potentials of several peaks were detected, such as at EC100 (Fig. 1), the fastest peak was accepted. The integrated EMG (iEMG) was calculated using the formula

$$iEMG[|m(t)|] = \int_0^t |m(t)|dt$$

where m is the raw EMG signal.

The iEMG was calculated at every channel, and the average iEMG was obtained from all channels without endplate zone.

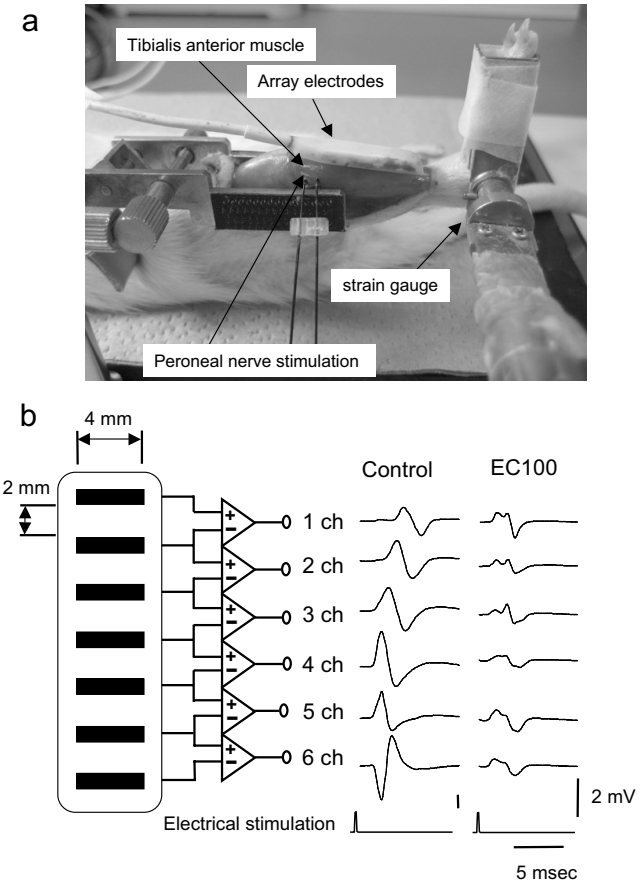

Fig. 1. A photograph shows experimental device and location of surface array electrode (**a**). Schematic illustration of surface array electrode (**b**) and raw action potential signals obtained from control and after 100 eccentric contractions (EC) of the TA muscles (**b**). At EC100, several peaks and a reduction of action potential amplitude were observed.

A recording of EMG and the isometric peak torque were obtained from 20 twitch contractions in each leg. The maximum correlation coefficient between two myoelectric signals of control muscle and EC muscle was calculated to clarify the waveform distortion of evoked myoelectric signals after the EC. To compare the signals in both control and damaged conditions, the signal of one channel chosen randomly (other than the motor end-plate zone) was used. For example, in Fig. 1, the signal of 2 channels in the control (left leg) was compared with the signal of 2 channels in EC100 (right leg) because the motor end-plate zone was recognized between 5 and 6 channels in control. The general calculation technique of MFCV by the correlation method [18] was applied to the calculation method of the maximum correlation coefficient in this study. Figure 2 shows an example of correlation coefficient plots between control and EC signal.

Histological evaluation. After the myoelectric signal protocols, the TA muscles of both legs were carefully dissected and the midbelly region was cut transversely to the long axis of the muscle. The tissue blocks were rapidly frozen in isopentane cooled by liquid nitrogen. Transverse 10 μm cross sections were made with a cryostat (Leica, CM1510, Germany) at –20°C and stained with hematoxylin-eosin (HE) to examine the histological features of muscle fiber damage. To avoid sampling bias, each section was subsampled at three different regions (anterior, central, posterior) so that these fields (total area = 2.13 mm^2) were analyzed per muscle. Muscle fiber damage was determined by a point-counting method using a 24 × 33 mounted grid (i.e., 792 points total; one square = 30 × 30 μm) on microscopic fields. Damaged fibers were defined as those with infiltration of inflammatory cells, pale staining of the cytoplasm, swollen appearance, or multiple central nuclei. Muscle damage was expressed as a percentage of counted grid squares. Quantitative analysis was performed in a blind manner and confirmed by another experienced investigator.

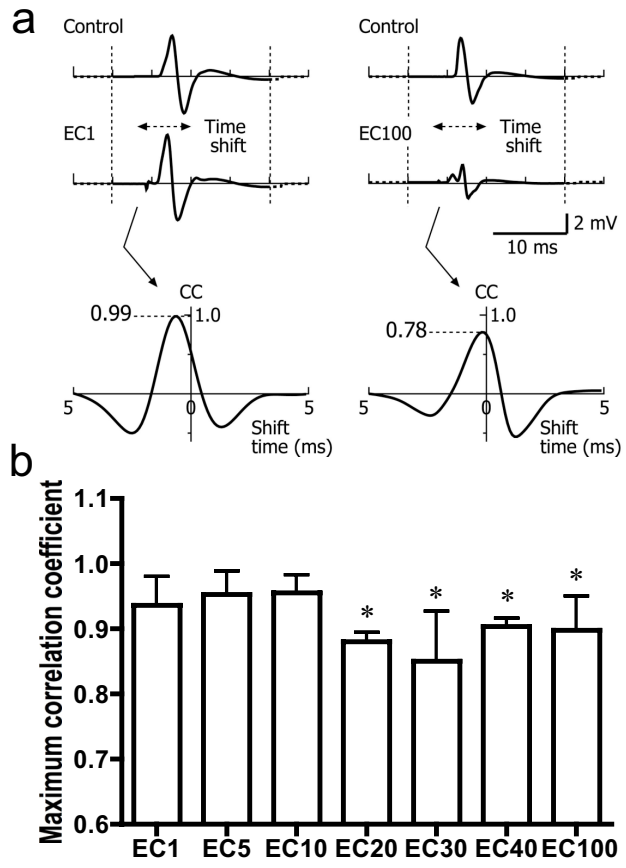

Fig. 2. Example of a correlation coefficient (CC) plot constructed from the time shift between two signals recorded 2 mm apart (**a**). Comparison of the maximum correlation coefficient (CC) of action potential waveform between control and eccentric muscle (**b**). Results are expressed as means ± SD. *$p < 0.05$ vs. EC10.

Statistical analysis. All experimental data are expressed as mean ± SD. All statistical analyses were performed in prism version 4.0 (GraphPad software Inc., USA). Group differences in MFCV, iEMG, and peak torque data were determined by a two-way analysis of variance (ANOVA, control vs. eccentric and number of contractions) and Bonferroni's post hoc test. Group differences in degree of muscle fiber damage and action potential waveform were analyzed by a one-way analysis of variance (ANOVA) and Bonferroni's post hoc test. The level of significance was set at $p < 0.05$.

RESULTS

An example of raw action potential signals obtained from control and EC100 is shown in Fig. 1. At EC100, several peaks and a reduction in amplitude of action potential were observed. Comparison of the correlation coefficient of action potential waveform is shown in Fig. 2. The correlation coefficient of a waveform was significantly lowered in the EC20 (0.88 ± 0.01), EC30 (0.85 ± 0.08), EC40 (0.90 ± 0.01), and 100EC (0.90 ± 0.05), compared with EC1 (0.94 ± 0.04), EC5 (0.95 ± 0.04), and EC10 (0.96 ± 0.03). These results identify a difference in the shape of the action potential between control and EC muscles.

The statistical significance of interaction effect was observed for peak torque and iEMG. The peak torque observed a significant reduction in groups more of than EC10 (EC1: 88.5%; EC5: 111.1%; EC10: 53.1%; EC20: 33.0%; EC30: 37.3%; EC40: 43.1%; EC100: 16.6% vs. contralateral control, Fig. 3). The iEMGs for EC20, EC30, and EC100 were significantly lower than control muscles (EC20: 44.1%; EC30: 33.3%; EC100: 23.1% vs. contralateral control, Fig. 3). MFCV did not differ between the TA muscles that received EC (3.52 to 4.51 m/s) and the contralateral control (3.76 to 4.19 m/s, Fig. 3). Histological examination of control muscles revealed no visible evidence of muscle tissue inflammation. In contrast, contracted muscles displayed mononuclear cell infiltration

with swollen appearances (Fig. 4). The TA muscles of EC1, EC5, and EC10 exhibited slight muscle damage; damaged muscle fibers constituted less than 3.9 ± 1.4% of total fibers (Figs. 3 and 4). On the other hand, TA muscles at EC20 (49.1 ± 6.8%), EC30 (60.6 ± 3.6%), EC40 (53.7 ± 15.6%), and EC100 (65.7 ± 6.1%) exhibited severe muscle damage (Figs. 3 and 4). Thus the extent of muscle damage increased precipitously at EC20. There was no significant difference in the percentage of muscle fibers damaged among the TA muscles of EC 20, EC30, EC40, and EC100 ($p > 0.05$).

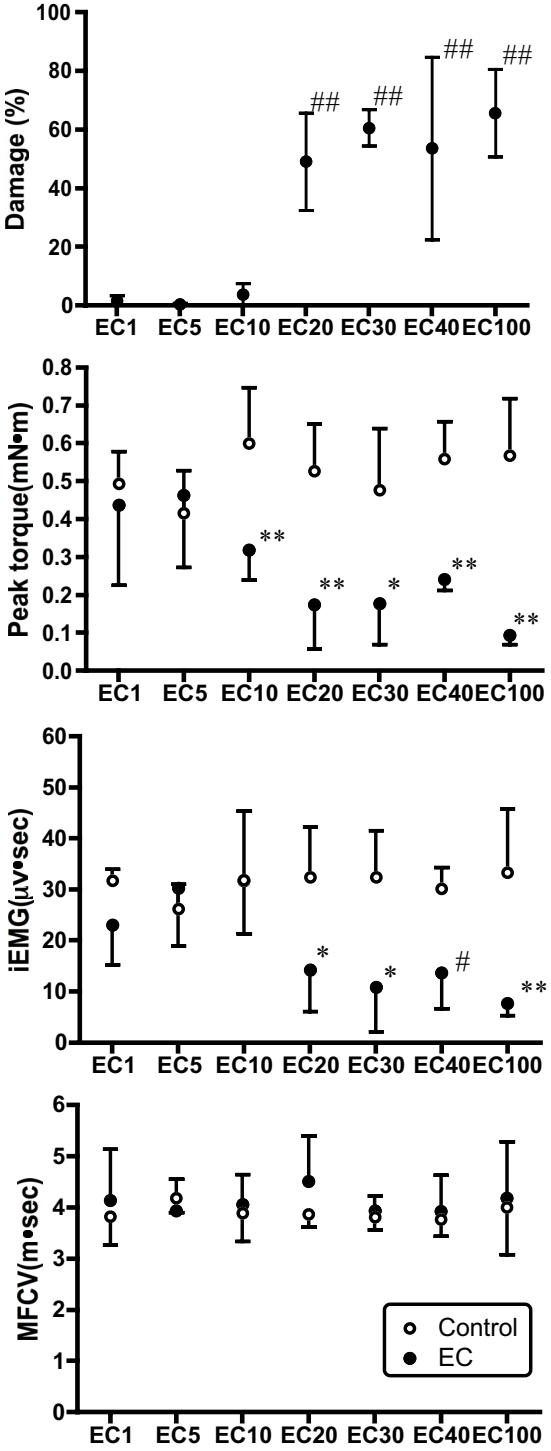

Fig. 3. Percentage of the damaged muscle fiber area isometric peak torque, integrated electromyogram (iEMG) and muscle fiber conduction velocity (MFCV) during twitch contraction after eccentric contractions (EC) at various numbers. Results are expressed as means ± SD. *$p < 0.05$ vs. Control, **$p < 0.01$ vs. Control, #$p = 0.06$ vs. Control, ##$p < 0.01$ vs. EC10.

DISCUSSION

The primary original finding of the present investigation is that the number of ECs is not a factor to determine the extent of histological muscle damage. Also, muscle damage occurred the modifications of the iEMG and action potential deformity. On the other hand, the propagation velocity of the action potential along muscle fiber (MFCV) was maintained for three days after the ECs.

Muscle damage

We find a nonlinear relationship between the number of muscle contractions and extent of muscle damage. As shown in Fig. 3, fewer than 10 repetitive contractions did not induce a significant increase in damaged muscle fiber. In about 20 repetitive contractions, however, the histological observation showed injury to 49% of the muscle cross-section area.

In contrast, Hesselink *et al.* [19] showed that the amount of histological muscle damage increases progressively with the number of forced lengthening contractions (60 to 300). This discrepancy may be attributed to differences in the velocity of lengthening contractions. Previous studies have reported that muscle damage is dependent on the speed of extension [20, 21]. The velocity of lengthening used in this study (angular velocity of 260 degree s^{-1}) was high compared with Hesselink's study (167 degree s^{-1}). Hesselink *et al.* [19] found no degenerative changes in muscles that were subjected to 60 contractions. These results suggest that muscle fiber may have a number of muscle contraction threshold to damage when an eccentric contraction is imposed with high velocity.

MFCV and action potential waveform

The MFCV depends on many factors, including the muscle-fiber type, cross-sectional area [22], and muscle temperature [23, 24]. However, the effect of muscle damage on the action potential propagation velocity is unknown. EC-induced muscle damage is accompanied with hypercontracture and edema of muscle fibers [16, 25]. The preset study clarified that severe muscle damage did not change MFCV during evoked twitch contraction. There is a possibility that muscle fiber of the state of edema does not participate in the recruitment of a motor unit. Most damaged fibers appeared to be in a necrotic condition with pronounced macrophage infiltration, as shown in Fig. 4. This observation is consistent with a previous

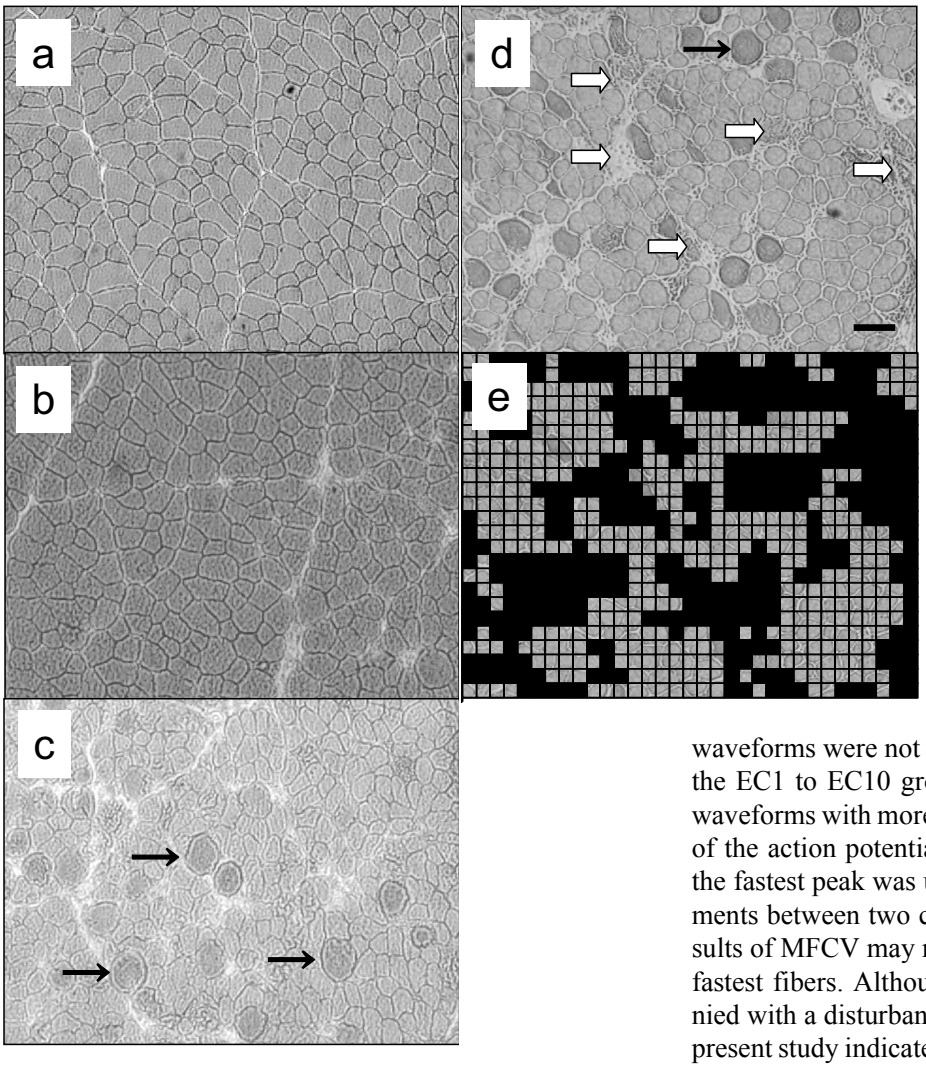

Fig. 4. Light micrographs of transversely sectioned TA muscle for control (**a**), 10 eccentric contractions (EC10) (**b**), 20 eccentric contractions (EC20) (**c**), and 100 eccentric contractions (EC100) (**d**). Bar = 50 μm. After eccentric muscle contraction, evidence of muscle fiber hypercontracture (➡) and leukocytic infiltration (⇨) was found in groups EC20 through EC100. The damaged area (black grid squares) **e** corresponding with **d** is shown.

study, which demonstrated that more macrophages invaded myocytes a few days after EC [26]. It is very likely that such necrotic muscle fibers could not be recruited during electrically elicited contractions.

Also, the results of MFCV in the present study may have been associated with the muscle fiber composition of tibialis anterior (TA) muscle. It is suggested that EC-induced muscle damage of type IIB fibers were preceded by other muscle-fiber types [16, 27]. Type IIB muscle fibers have specific components by the high frequency of power spectrum. Thus selective muscle-fiber damage of the fast type could produce changes in the shift of the power spectrum of EMG to a low frequency [11, 12, 14]. Although the myosin heavy chain isoforms (MHC) of rat TA are a heterogeneous composition that contain ~5% type I, ~15% type IIA, and ~70% IIX and/or IIB MHC [28], the muscle composition of rat TA is predominantly type II fiber. Therefore the MFCV results obtained by the present study might possibly be caused by muscle composition of rat TA.

It may be necessary to consider the calculation methods of MFCV. Several peaks and distortions of action potential waves were found in damaged muscle, but these waveforms were not observed in all control muscles or in the EC1 to EC10 groups (Fig. 2). It is possible that the waveforms with more peaks mean a dispersion of velocity of the action potential among individual fibers. Because the fastest peak was used as the time difference measurements between two channels in the present study, the results of MFCV may reflect the conduction velocity of the fastest fibers. Although the muscle damage is accompanied with a disturbance of waveforms (Figs. 1 and 2), the present study indicated that healthy muscle fibers or intact segments of damaged fibers maintain normal velocity of propagation. Previous studies indicate that conductivity of muscle tension was maintained in the focally damaged fibers [29, 30]. Therefore the focally damaged fibers may be characterized by the maintenance of propagation of action potentials and the conductivity of muscle tension.

iEMG and isometric strength

Decrement in maximal isometric strength is one of several sequelae that typically follow EC [31, 32]. Warren *et al.* [32] reported that the decline of peak isometric force after EC elicited by tetanic and twitch conditions were –42.6% and –55.6%, respectively. In this study, decrement in peak isometric force during twitch was observed for muscle in the EC10 (53.1% vs. control) to EC100 (16.6% vs. control) groups. The force loss in the present investigation cannot be explained completely by changes in iEMG or the extent of histological muscle damage. Specifically, in the EC10 leg a significant decline of muscle force was present concomitant with an unchanged iEMG and low histological damage by HE stain (under 4%). Previous studies suggested that the fall in muscle force after EC can be attributed to the disruption of sarcomeres in

myofibrils and the damage to excitation-contraction (E-C) coupling [33]. If the muscle fiber damage was intensive enough, the fiber would lead to a local inflammation with tissue swelling. However, when muscle damage is not sufficient, no necrosis of muscular fiber occurs, but force output would lead to decline. Although the damage at the myofibril level could not be observed with a light microscope, myofibril damage such as sarcomere disruption would occur in the EC10. Another effect attributed to the force drop after EC is the force–frequency relationship shift with muscle damage [34]. Twitch force was used as the index of muscle damage in this study. Therefore a decline of twitch force in the EC10 group would be expected to collapse the myofibril structure.

Consideration of an experimental model

Interpretation of iEMG and MFCV after ECs required consideration of the phase of cellular response to muscle damage. For example, in the early phase following EC, focal degenerative and inflammatory responses in damaged muscle fiber are accompanied by alteration of membrane depolarization [35] and fiber edema [16]. Previous studies [26, 36] also demonstrated the presence of necrotic muscle fibers with macrophage invasion at 1 to 3 days after injury and muscle fiber regeneration with myoblasts and myotubes at 4 days after [37]. These physiological and structural changes may contribute to the determination of EMG parameters. In human studies, the median frequency of the power spectrum decreased immediately after EC, and this modification was still present at one week [11]. It remains unclear whether the structural status of muscle from the injury-to-recovery period influences EMG parameters. Further research is needed to establish the time course of the relationship between EMG modifications and muscle damage.

In conclusion, although different numbers of ECs were adopted, the degree of histological muscle damage was almost the same when damage was present, which was accompanied with decreased iEMG and a change of action potential waveform. However, MFVC and isometric peak torque are not consistently related to histological muscle damage.

The present study was supported partially by Casio Science Promotion Foundation. We gratefully acknowledge Dr. D. C. Poole at Kansas State University for helpful comments on the manuscript and Dr. T. Masuda at Tokyo Medical and Dental University, Mr. Y. Fukurotani, Mr. K. Hirabayashi, Mr. T. Onodera, and Mr. N. Yamada for excellent technical support.

REFERENCES

1. Enoka RM. Eccentric contractions require unique activation strategies by the nervous system. J Appl Physiol. 1996;81:2339-46.
2. Clarkson PM, Hubal MJ. Exercise-induced muscle damage in humans. Am J Phys Med Rehabil. 2002;81:S52-69.
3. Proske U, Morgan DL. Muscle damage from eccentric exercise: mechanism, mechanical signs, adaptation and clinical applications. J Physiol. 2001;537:333-45.
4. Enoka RM, Stuart DG. Neurobiology of muscle fatigue. J Appl Physiol. 1992;72:1631-48.
5. Hägg GM. Interpretation of EMG spectral alterations and alteration indexes at sustained contraction. J Appl Physiol. 1992;73:1211-7.
6. Masuda K, Masuda T, Sadoyama T, Inaki M, Katsuta S. Changes in surface EMG parameters during static and dynamic fatiguing contractions. J Electromyogr Kinesiol. 1999;9:39-46.
7. Bigland-Ritchie B, Donovan EF, Roussos CS. Conduction velocity and EMG power spectrum changes in fatigue of sustained maximal efforts. J Appl Physiol. 1981;51:1300-5.
8. Cruz-Martínez A, Ramírez A, Arpa J. Quadriceps atrophy after knee traumatisms and immobilization: electrophysiological assessment. Eur Neurol. 2000;43:110-4.
9. Van der Hoeven JH, Zwarts MJ, Van Weerden TW. Muscle fiber conduction velocity in amyotrophic lateral sclerosis and traumatic lesions of the plexus brachialis. Electroencephalogr Clin Neurophysiol. 1993;89:304-10.
10. Chen TC. Effects of a second bout of maximal eccentric exercise on muscle damage and electromyographic activity. Eur J Appl Physiol. 2003;89:115-21.
11. Day SH, Donnelly AE, Brown SJ, Child RB. Electromyogram activity and mean power frequency in exercise-damaged human muscle. Muscle Nerve. 1998;21:961-3.
12. Felici F, Colace L, Sbriccoli P. Surface EMG modifications after eccentric exercise. J Electromyogr Kinesiol. 1997;7:193-202.
13. Kroon GW, Naeije M. Recovery of the human biceps electromyogram after heavy eccentric, concentric or isometric exercise. Eur J Appl Physiol Occup Physiol. 1991;63:444-8.
14. Sbriccoli P, Felici F, Rosponi A, Aliotta A, Castellano V, Mazzà C *et al.* Exercise induced muscle damage and recovery assessed by means of linear and non-linear sEMG analysis and ultrasonography. J Electromyogr Kinesiol. 2001;11:73-83.
15. Berry CB, Moritani T, Tolson H. Electrical activity and soreness in muscles after exercise. Am J Phys Med Rehabil. 1990;69:60-6.
16. Kano Y, Sampei K, Matsudo H. Time course of capillary structure changes in rat skeletal muscle following strenuous eccentric exercise. Acta Physiol Scand. 2004;180:291-9.
17. Nishizono H, Saito Y, Miyashita M. The estimation of conduction velocity in human skeletal muscle in situ with surface electrodes. Electroencephalogr Clin Neurophysiol. 1979;46:659-64.
18. Mito K, Sakamoto K. On the evaluation of muscle fiber conduction velocity considering waveform properties of an electromyogram in M. biceps brachii during voluntary isometric contraction. Electromyogr Clin Neurophysiol. 2002;42:137-49.
19. Hesselink MK, Kuipers H, Geurten P, Van Straaten H. Structural muscle damage and muscle strength after incremental number of isometric and forced lengthening contractions. J Muscle Res Cell Motil. 1996;17:335-41.
20. Fridén J, Lieber RL. Structural and mechanical basis of exercise-induced muscle injury. Med Sci Sports Exerc. 1992;24:521-30.
21. McCully KK, Faulkner JA. Characteristics of lengthening contractions associated with injury to skeletal muscle fibers. J Appl Physiol. 1986;61:293-9.
22. Kupa EJ, Roy SH, Kandarian SC, De Luca CJ. Effects of muscle fiber type and size on EMG median frequency and conduction velocity. J Appl Physiol. 1995;79:23-32.
23. Gray SR, De Vito G, Nimmo MA, Farina D, Ferguson RA. Skeletal muscle ATP turnover and muscle fiber conduction velocity are elevated at higher muscle temperatures during maximal power output development in humans. Am J Physiol Regul Integr Comp Physiol. 2006;290:R376-82.
24. Jarcho LW, Berman B, Dowben RM, Lilienthal JL Jr. Site of origin and velocity of conduction of fibrillary potentials in denervated skeletal muscle. Am J Physiol. 1954;178:129-34.
25. Fridén J, Lieber RL. Segmental muscle fiber lesions after repetitive eccentric contractions. Cell Tissue Res. 1998;293:165-71.
26. Pizza FX, Koh TJ, McGregor SJ, Brooks SV. Muscle inflammatory cells after passive stretches, isometric contractions, and lengthening contractions. J Appl Physiol. 2002;92:1873-8.
27. Lieber RL, Fridén J. Selective damage of fast glycolytic muscle fibres with eccentric contraction of the rabbit tibialis anterior. Acta Physiol Scand. 1988;133:587-8.
28. Roy RR, Zhong H, Siengthai B, Edgerton VR. Activity-dependent influences are greater for fibers in rat medial gastrocnemius than tibialis anterior muscle. Muscle Nerve. 2005;32:473-82.
29. Street SF. Lateral transmission of tension in frog myofibers: a myofibrillar network and transverse cytoskeletal connections are possible transmitters. J

Cell Physiol. 1983;114:346-64.
30. Wang K, Ramirez-Mitchell R. A network of transverse and longitudinal intermediate filaments is associated with sarcomeres of adult vertebrate skeletal muscle. J Cell Biol. 1983;96:562-70.
31. Proske U, Allen TJ. Damage to skeletal muscle from eccentric exercise. Exerc Sport Sci Rev. 2005;33:98-104.
32. Warren GL, Lowe DA, Hayes DA, Karwoski CJ, Prior BM, Armstrong RB. Excitation failure in eccentric contraction-induced injury of mouse soleus muscle. J Physiol. 1993;468:487-99.
33. Warren GL, Ingalls CP, Lowe DA, Armstrong RB. Excitation-contraction uncoupling: major role in contraction-induced muscle injury. Exerc Sport Sci Rev. 2001;29:82-7.
34. Newham DJ, Mills KR, Quigley BM, Edwards RH. Pain and fatigue after concentric and eccentric muscle contractions. Clin Sci (Lond). 1983;64:55-62.
35. McBride TA, Stockert BW, Gorin FA, Carlsen RC. Stretch-activated ion channels contribute to membrane depolarization after eccentric contractions. J Appl Physiol. 2000;88:91-101.
36. Frenette J, Cai B, Tidball JG. Complement activation promotes muscle inflammation during modified muscle use. Am J Pathol. 2000;156:2103-10.
37. McCully KK, Faulkner JA. Injury to skeletal muscle fibers of mice following lengthening contractions. J Appl Physiol. 1985;59:119-26.